First Experimental Demonstration of a Plasmonic MMI Switch in 10 Gb/s True Data Traffic Conditions

D. Kalavrouziotis[(1)], S. Papaioannou[(2,3)], K. Vyrsokinos[(3)], L. Markey[(4)], Alain Dereux[(4)], G. Giannoulis[(1)], D. Apostolopoulos[(1)], H. Avramopoulos[(1)] and N. Pleros[(2,3)]

[(1)] School of Electrical and Electronic Engineering, National Technological University of Athens, Greece, dkalav@mail.ntua.gr.
[(2)] Department of Informatics, Aristotle University of Thessaloniki, Greece.
[(3)] Informatics and Telematics Institute, Center for Research and Technology Hellas, Greece.
[(4)] Institute Carnot de Bourgogne, University of Burgundy, France.

Abstract *We report the first experimental performance evaluation of a 75 um long plasmonic MMI switch, hetero-integrated on a SOI platform, operating with 10Gb/s data signals. The switch exhibits 2.9μs response time and 44.5% modulation depth while its extinction ratio varies from 5.4 to -1.5 dB for 35mW switching power. Error-free performance was achieved.*

Introduction

Optical interconnects have recently made their appearance as a much promising candidate for ensuring technological gateways to short-range and even chip-scale communications[1]. In particular, hybrid on-chip opto-electronic routing fabrics with optical switching elements controlled by electronic signals have attracted the interest of the scientific community as they provide significant power consumption and performance benefits[2]. In this frame, the discipline of plasmonics has raised a great promise for additional energy consumption savings instigated by the intrinsic metal-polymer interface of plasmonic waveguides that provides a "natural" energy-efficient platform for merging broadband optical links with intelligent electronic processing, enabling low-power and small-footprint active functional circuitry[3,4].

The recent progress on active plasmonic switches relies on the advantages of the Dielectric Loaded Surface Plasmon Polariton (DLSPP) waveguide configuration combined with the thermo-optic (TO) effect as the mature plasmonic manipulation mechanism. Lately, a Polymethylmethacrylate (PMMA)-loaded SPP racetrack resonator requiring only 3.3mW[5] of power has been presented while an active PMMA-loaded SPP-based A-MZI switch employing 90μm plasmonic arms operating with 10Gb/s optical data traffic, has signified the first successful experimental evaluation of an active DLSPP configuration in true data traffic environments[6]. Moreover, theoretical studies[7] as well as recently published Leakage Radiation Microscopy characterization results of a Dual Mode Interference switch[8], demonstrate the potential of plasmonic Multi Mode Interference (MMI) structures to be deployed in low-power and reduced-footprint switching configurations.

In this manuscript, we report the first experimental TO switching operation of a DLSPP-based MMI structure, with a total footprint of 0.001 mm^2, in 10Gb/s data traffic conditions. The TO response of the device is characterized in dynamic operation, showing a 44.5% modulation depth with 2.9 μs rise- and 4 μs fall-time while its system-level credentials are presented at 10 Gb/s yielding successful switching operation with extinction ratio (ER) varying from 5.4 to -1.5 dB for 35 mW switching power. Finally, error-free performance in both ON and OFF states with negligible power penalty at 10^{-9} Bit-Error-Rate (BER) value is demonstrated.

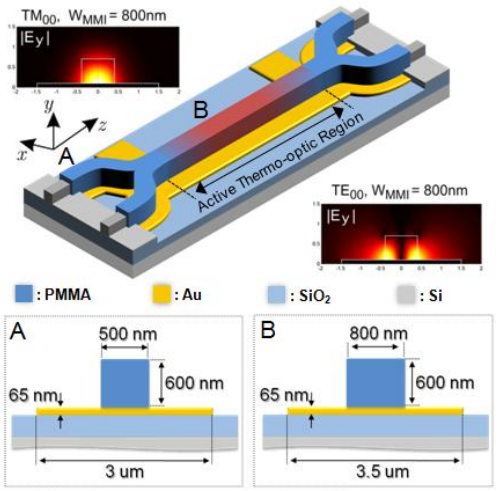

Fig. 1: Si – DLSPP MMI switch and waveguide crossections

Experimental Setup

The plasmonic MMI switching structure is depicted in Fig. 1. It comprises of two PMMA-loaded SPP waveguides (section A) coupled into a 75-μm-long PMMA-loaded MMI section, serving as the active thermo-optic region (section B). The DLSPP waveguides consist of 65-nm-thick and 3-μm-wide gold stripes on top of which dielectric PMMA ridges with cross-

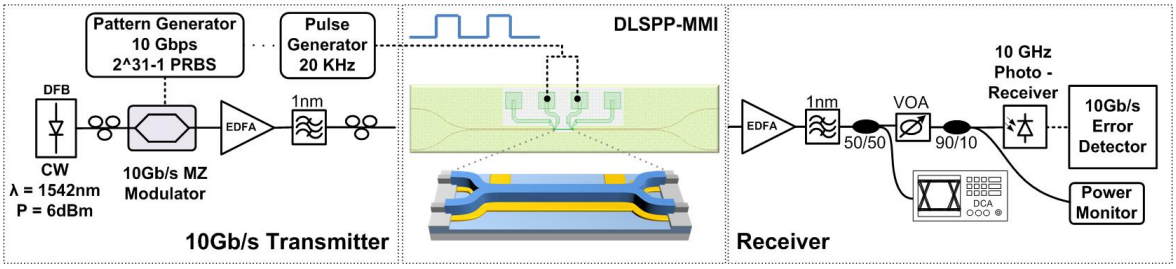

Fig. 2: Experimental Setup

sections of 500×600 nm^2 were placed. The MMI section is formed by an 800x600 nm^2 PMMA ridge lying on a 65-nm-thick and 3.5-μm-wide gold stripe. The width of the PMMA ridge was chosen so that the MMI section supports the fundamental (symmetric) and one higher order (anti-symmetric) mode[7], as shown in Fig. 1. Switching operation is achieved via the thermo-optic control of the modes' beating length (active thermo-optic region) of the MMI[7], which is realized by current injection through electrical contact pads into the gold stripe under the MMI section.

The total footprint of the DLSPP MMI switch was 1056 μm^2 and it was hetero-integrated on a Silicon-on-Insulator (SOI) platform employing 400×340 nm^2 silicon rib waveguides and TM grating couplers for the in/out light coupling. A detailed description of the heterointegration process as well as the SOI rib waveguide platform hosting the plasmonic elements is described in [5].

Fig. 2 illustrates the experimental setup. A continuous wave (CW) signal at 1542 nm was launched into a Ti:$LiNbO_3$ Mach-Zehnder modulator driven by a pseudo-random bit sequence (PRBS) pattern generator, yielding a 10 Gb/s 2^{31}-1 (and 2^7-1) non-return-to-zero (NRZ) data sequence at its output. The modulated signal was then amplified, using a high-power erbium-doped fiber amplifier (EDFA) providing 26 dBm output power, filtered and launched into the MMI switch. The total fiber-to-fiber losses of the device were found to be 45.4 dB, 29 dB of them coming from the SOI input/output grating couplers, 2.4 dB owing to silicon propagation losses, 8 dB due to plasmonic propagation losses and 6 dB stemming from the Si-to-DLSPP coupling interfaces. The MMI's output signal was amplified in a low-noise EDFA, filtered, split and then fed simultaneously into a 30 GHz sampling oscilloscope and a 10 GHz photo-receiver that was connected to an error detector. The control signal of the switch was provided by a pulse generator operating at 20 KHz that was directly connected to the electrical pads.

Results and Discussion

The MMI switching element was experimentally characterized in both static and dynamic operation (Fig. 3). For the static characterization, a CW signal of 6 dBm at 1542nm was used as input signal while a direct current (DC) source, connected to the metal pads of the structure, was used to generate the control signal. Fig. 3(a) depicts the output power of the switch at the BAR and CROSS ports plotted against the applied current. The graph reveals that for the 0 to 30 mA current range, the output power at the CROSS port is constant while the power at the BAR port drops by 1.2 dB. In addition, for an applied current of 30 to 50 mA, the BAR port output power is increased by

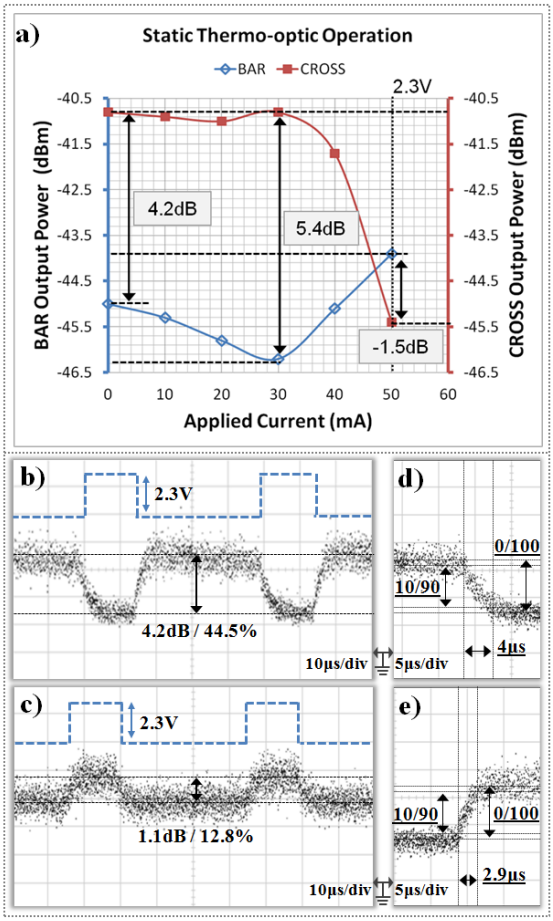

Fig. 3: (a) Static TO characterization of the MMI switch, (b) CROSS and (c) BAR output for dynamic TO operation, (d) rise and (e) fall times (CROSS port, 10% - 90%)

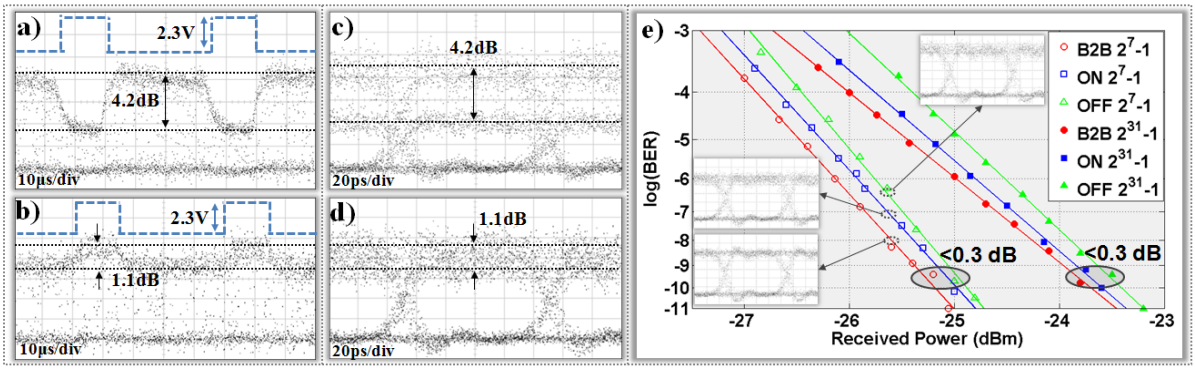

Fig. 4: 10Gb/s data trace at the (a) CROSS and the (b) BAR port, (c) 10Gb/s eye diagram at the CROSS port, (d) 10Gb/s eye diagram at the BAR port, (e) BER curves for 31st and 7th order data patterns and corresponding eye diagrams (insets)

2.3 dB while the CROSS port output power is decreased by 4.2 dB. The static ER of the MMI switch is found to be 4.2 dB for 0 mA, 5.4 dB for 30 mA and -1.5 dB for 50 mA injected current, with the negative operator indicating the change of the dominant output port.

Fig. 3(b)-(c) show the response of the device when operated in dynamic conditions with CW input and 20 KHz rectangular pulses of 15 µs duration and 50 mA peak current as the control signal. The oscilloscope traces in Fig. 3(b)-(c) indicate complementary operation with 12.8% and 44.5% modulation depth for the BAR and CROSS ports, respectively. The rising and falling edges of the CROSS port revealed 2.9 µs rise and 4µs fall time, as shown in Fig. 3 (d) -(e). It should be noted that according to the static TO behavior of the device, optimum switching operation would have been obtained if the MMI was biased at 30 mA and driven with 30 mA pulses or more. However, this was highly prohibited by the low service temperature of PMMA that limited the maximum operational current to 50 mA. The total power consumption of the device was 115mW, with only 35mW owing to the metal stripe of the active region.

The performance of the switch was also evaluated with 10 Gb/s NRZ optical data signals. The control signal consisted again of 15 µs electrical pulses at 20 KHz repetition rate. Fig. 4(a) presents a snapshot of the 10Gb/s signal's trace exiting the CROSS port compared to the applied control pulses (blue dashed line) while Fig. 4(b) shows the corresponding trace for the BAR port. The eye diagrams of the CROSS and BAR output signals, shown in Fig. 4(c)-(d), comprise two "1" levels, one for the switched and one for the un-switched state, respectively. The difference between those two levels reveals an ER value of 4.2 dB for the CROSS port and 1.1 dB for the BAR port, values that are in agreement with the outcomes of the initial static characterization.

Fig. 4(e) shows the BER measurements that have been performed in order to evaluate the MMI's effect on the signal integrity in both ON (50 mA current) and OFF (0 mA current) states for 10 Gb/s 2^7-1 and 2^{31}-1 PRBS data streams. Both the CROSS-port during OFF- and the BAR-port during ON-state operation exhibit error-free performance with less than 0.3 dB power penalty (at 10^{-9} BER value) against the back-to-back (B2B) measurements.

Conclusions

We have demonstrated a TO plasmonic MMI switch operating with 10Gb/s data traffic signals. Dynamic device operation with 2.9 µs response time and 44.5% modulation depth was achieved, requiring 35 mW of electrical power, while error-free performance with negligible power penalty has been presented. Even though, high-quality performance was hindered by the poor TO coefficient of PMMA, significant improvement is expected through the exploitation of more advanced polymers as the dielectric loadings[7,8].

Acknowledgements

This work was partially supported by the European FP7 ICT-PLATON (ICT- STREP no. 249135) project.

References

[1] M.A.Taubenblatt et al., Proc. OFC'11, OThH3 (2011).

[2] K. Bergman, in Proc. ECOC'06, Tu1.2.1, (2006).

[3] H. A. Atwater, Sci. Am. Mag, **296** (2007).

[4] R.Zia et al., Mater. Today **9**, 7 (2006).

[5] G. Giannoulis et al. IEEE Photon. Technol. Lett. **24**, 5 (2012).

[6] D. Kalavrouziotis et al., Proc. OFC'12, OW3E.3 (2012).

[7] A. Pitilakis et al., J. Lightwave Technol. **29**, 17 (2011).

[8] J.C Weeber et al., Appl. Phys. Lett **99**, 24 (2011)